microbial biotechnology

Open Access

Identification of essential β-oxidation genes and corresponding metabolites for oestrogen degradation by actinobacteria

Tsun-Hsien Hsiao,[1,†] Tzong-Huei Lee,[2,†] Meng-Rong Chuang,[1] Po-Hsiang Wang,[3,4] Menghsiao Meng,[5] Masae Horinouchi,[6] Toshiaki Hayashi,[7] Yi-Lung Chen[8] and Yin-Ru Chiang[1]

[1]*Biodiversity Research Center, Academia Sinica, Taipei, 115, Taiwan.*
[2]*Institute of Fisheries Science, National Taiwan University, Taipei, 106, Taiwan.*
[3]*Gradaute Institute of Environmental Engineering, National Central University, Taoyuan, 320, Taiwan.*
[4]*Earth-Life Science Institute (ELSI), Tokyo Institute of Technology, Tokyo, Japan.*
[5]*Graduate Institute of Biotechnology, National Chung Hsing University, Taichung, 402, Taiwan.*
[6]*Condensed Molecular Materials Laboratory, RIKEN, Saitama, 351-0198, Japan.*
[7]*Environmental Molecular Biology Laboratory, RIKEN, Saitama, 351-0198, Japan.*
[8]*Department of Microbiology, Soochow University, Taipei, 111, Taiwan.*

Summary

Steroidal oestrogens (C_{18}) are contaminants receiving increasing attention due to their endocrine-disrupting activities at sub-nanomolar concentrations. Although oestrogens can be eliminated through photodegradation, microbial function is critical for removing oestrogens from ecosystems devoid of sunlight exposure including activated sludge, soils and aquatic sediments. Actinobacteria were found to be key oestrogen degraders in manure-contaminated soils and estuarine sediments. Previously, we used the actinobacterium *Rhodococcus* sp. strain B50 as a model microorganism to identify two oxygenase genes, *aedA* and *aedB*, involved in the activation and subsequent cleavage of the estrogenic A-ring respectively. However, genes responsible for the downstream degradation of oestrogen A/B-rings remained completely unknown. In this study, we employed tiered comparative transcriptomics, gene disruption experiments and mass spectrometry-based metabolite profile analysis to identify oestrogen catabolic genes. We observed the up-regulation of thiolase-encoding *aedF* and *aedK* in the transcriptome of strain B50 grown with oestrone. Consistently, two downstream oestrogenic metabolites, 5-oxo-4-norestrogenic acid (C_{17}) and 2,3,4-trinorestrogenic acid (C_{15}), were accumulated in *aedF*- and *aedK*-disrupted strain B50 cultures. Disruption of *fadD3* [3aα-H-4α(3'-propanoate)-7aβ-methylhexahydro-1,5-indanedione (HIP)-coenzyme A-ligase gene] in strain B50 resulted in apparent HIP accumulation in oestrone-fed cultures, indicating the essential role of *fadD3* in actinobacterial oestrogen degradation. In addition, we detected a unique *meta*-cleavage product, 4,5-*seco*-estrogenic acid (C_{18}), during actinobacterial oestrogen degradation. Differentiating the oestrogenic metabolite profile and degradation genes of actinobacteria and proteobacteria enables the cost-effective and time-saving identification of potential oestrogen degraders in various ecosystems through liquid chromatography–mass spectrometry analysis and polymerase chain reaction-based functional assays.

Received 23 April, 2021; accepted 1 September, 2021.
For correspondence. *E-mail yilungchen@scu.edu.tw; Tel. 886-2-28819471 (ext. 6856); Fax 886-2-28819471 (ext. 6879). **E-mail yinru915@gate.sinica.edu.tw; Tel. 886-2-27872251; Fax 886-2-27899624.
[†][†]T.-H. Hsiao and T.-H. Lee contributed equally to this work.
Microbial Biotechnology (2022) **15**(3), 949–966
doi:10.1111/1751-7915.13921
Funding information
This study was supported by the Ministry of Science and Technology of Taiwan (109-2221-E-001-002, 109-2811-B-001-513 and 110-2311-B-031-001) and Academia Sinica Career Development Award (AS-CDA-110-L13). Po-Hsiang Wang was supported by the Research and Development Office as well as Research Center for Sustainable Environmental Technology, National Central University, Taiwan.

Introduction

Steroidal oestrogens regulate the development of the reproductive system and secondary sex characteristics of vertebrates. The synthesis and secretion of oestrogens exclusively occur in animals, particularly in vertebrates such as humans and livestock (Matsumoto *et al.*, 1997; Tarrant *et al.*, 2003). In the liver, oestrogens undergo structural modifications (conjugation with glucuronate or sulphate) and are converted into more soluble products for subsequent excretion (Harvey and

Ferrier, 2011). In the environment, these conjugated oestrogens are often hydrolysed by microorganisms to form free oestrogens (Koh *et al*., 2008). Chronic exposure to trace oestrogens at sub-nanomolar levels can disrupt the endocrine system and sexual development in higher animals, particularly aquatic species (Belfroid *et al*., 1999; Baronti *et al*., 2000; Huang and Sedlak, 2001; Kolodziej *et al*., 2003; Lee *et al*., 2006). For example, the EC50 of 17β-estradiol (E2) that causes infertility in fathead minnows (*Pimephales promelas*) is 120 ng l^{-1} (Kramer *et al*., 1998). In addition, oestrogens have been classified as Group 1 carcinogens by the World Health Organization (Agents classified by the *IARC Monographs*, *Volumes 1–129*). However, a recent study argued that invertebrates incapable of synthesizing oestrogens are not affected by environmental oestrogens (Balbi *et al*., 2019).

Concern is increasing about the role of oestrogens as a contaminant that poses a public health challenge to municipalities due to the increasing human population and mounting demand for livestock products. Livestock manure (Hanselman *et al*., 2003) and municipal sewage-derived fertilizers (Lorenzen *et al*., 2004; Hamid and Eskicioglu, 2012) are major sources of environmental oestrogens, whereas anaerobic digestion processes do not appear to alter the total oestrogen concentration (< 10%) in livestock manure (Noguera-Oviedo and Aga, 2016). Oestrogens in sludges may be released to aquatic ecosystems through rainfall and leaching (Hanselman *et al*., 2003; Kolodziej *et al*., 2004).

Both natural oestrogens [e.g. oestrone (E1) and E2] and synthetic oestrogens (e.g. 17α-ethynylestradiol) can be photodegraded in surface water ecosystems with a degradation half-live ranging from days to weeks (Jurgens *et al*., 2002; Lin and Reinhard, 2005). However, photodegradation rarely occurs in environments such as sludge, soils and aquatic sediments that do not receive sunlight exposure. Alternatively, microbial degradation is a major mechanism for removing oestrogens from these environment (Thayanukul *et al*., 2010; Chen *et al*., 2017; 2018; Chiang *et al*., 2020; Wang *et al*., 2020). Common bacterial taxa capable of complete oestrogen degradation include actinobacteria, such as *Nocardia* sp. strain E110 (Coombre *et al*., 1966) and *Rhodococcus* spp. (Yoshimoto *et al*., 2004; Kurisu *et al*., 2010; Hsiao *et al*., 2021), and proteobacteria, such as *Novosphingobium tardaugens* (Fujii *et al*., 2002), *Novosphingobium* spp. (Chen *et al*., 2018; Wu *et al*., 2019; Li *et al*., 2021), *Sphingobium estronivorans* (Qin *et al*., 2020) and *Sphingomonas* spp. (Ke *et al*., 2007; Yu *et al*., 2007; Chen *et al*., 2017). Several possible oestrogen biodegradation pathways have been proposed (Yu *et al*., 2013; Chiang *et al*., 2020; Li *et al*., 2021), suggesting that bacteria in different taxa likely adopt multiple strategies to degrade oestrogens. The results of gene disruption experiments and enzyme characterization have indicated that proteobacteria adopt the cytochrome P450-type monooxygenase EdcB (oestrone 4-hydroxylase; Ibero *et al*., 2020) and the type I extradiol dioxygenase OecC (4-hydroxyestrone 4,5-dioxygenase; Chen *et al*., 2017) to activate and cleave the oestrogenic A-ring. Recently, we demonstrated that actinobacteria use a similar strategy to cleave the oestrogenic A-ring with functionally homologous enzymes exhibiting a sequence identity of < 40% for proteobacterial enzymes. However, essential genes involved in the downstream steps of both actinobacterial and proteobacterial degradation pathways remain unknown.

In this study, we used the actinobacterium *Rhodococcus* sp. strain B50, a soil isolate, as the model microorganism to identify downstream metabolites and catabolic genes because of its excellent efficiency in oestrogen degradation and its compatibility with commercial genetic manipulation techniques. On the basis of the annotated strain B50 genome (Hsiao *et al*., 2021), we performed tiered comparative transcriptomics, gene disruption experiments and metabolite profile analysis to elucidate the actinobacterial oestrogen degradation pathway.

Results

Identification of strain B50 genes involved in oestrogen degradation through comparative transcriptomic analysis

We first employed comparative transcriptomics to probe genes differentially expressed under E1-fed conditions. In addition to the degradation of oestrogens such as E1 and E2, strain B50 can degrade other steroids such as testosterone and cholesterol. Therefore, we used the transcriptomes of strain B50 grown on cholesterol and testosterone as controls for the comparative transcriptomics analysis. Consistent with the observed phenotype, the strain B50 linear chromosome (GMFMDNLD 2) contains a complete set of cholesterol/androgen degradation genes in the established 9,10-*seco* pathway (Holert *et al*., 2016; Crowe *et al*., 2018) including genes involved in cholesterol uptake (*mce4* genes; GMFMDNLD_02935 to 02949), steroidal side-chain degradation (GMFMDNLD_02968 to 02992 and GMFMDNLD_03076 to 03082), androgenic A/B-rings degradation (GMFMDNLD _03002 to 03014 and GMFMDNLD _03061 to 03069) and steroidal C/D-rings degradation (GMFMDNLD _03017 to 03024 and GMFMDNLD _03033 to 03050; Dataset S1). Among them, we identified *fadD3* (HIP-CoA-ligase gene; GMFMDNLD_03043) as being responsible for steroidal C-rings degradation.

In our previous study (Hsiao *et al*., 2021), we identified the *aed* gene cluster containing two oxygenase genes, *aedA* and *aedB*, that is located in the megaplasmid of strain B50. Here, we investigated whether *aed* genes

are induced by oestrogens. We grew strain B50 cells by using three steroid substrates, namely E1, testosterone or cholesterol. Subsequently, we performed a comparative transcriptomic analysis to detect genes specifically up-regulated in the E1-fed culture (Fig. 1). As expected, *mce4* genes (GMFMDNLD_02935 to 02949) were apparently up-regulated only under cholesterol-fed conditions (Fig. 1A). Our data indicated that genes involved in steroidal C- and D-rings are expressed at similar levels (< 4-fold difference) in all three treatments (Fig. 1). By contrast, the *aed* gene cluster (GMFMDNLD _05332 to 05349) was differentially up-regulated (> 5-fold difference) in the E1-fed culture (Fig. 1; Dataset S1). In addition to GMFMDNLD _05336 and GMFMDNLD _05338 encoding AedA and AedB, respectively (Hsiao *et al.*, 2021), in the *aed* gene cluster, we identified a putative medium-chain fatty acid:CoA-ligase gene [GMFMDNLD _05341 (*aedJ*)]. Moreover, genes encoding two sets of β-oxidation enzymes, including acyl-CoA dehydrogenase [GMFMDNLD _05345 (*aedN*) and 05347 (*aedP*)], enoyl-CoA hydratase [GMFMDNLD _05333 (*aedD*), 05344 (*aedM*) and 05346 (*aedO*)], 3-hydroxyacyl-CoA dehydrogenase [GMFMDNLD _05334 (*aedE*) and 05337 (*aedG*)] and thiolase [GMFMDNLD _05335 (*aedF*) and 05342 (*aedK*)], are present in this gene cluster (Fig. 2). Highly similar β-oxidation genes (with a deduced amino acid sequence identity > 70%) were also present in the genome of the oestrogen-degrading *Rhodococcus* sp. strain DSSKP-R-001 (Tian *et al.*, 2020; Hsiao *et al.*, 2021).

Among the characterized proteins, the strain B50 AedF and AedK exhibited highest sequence identity (39% and 43%) with the FadA5 and Ltp2 from *Mycobacterium tuberculosis* strain H37Rv respectively. Although the BLASTp (NCBI) analysis indicated that AedK contains a thiolase domain, the sequence alignment and phylogenetic analysis of the AedK suggested that it is likely an aldolase (Fig. S1). Both the actinobacterial enzymes FadA5 and Ltp2 contain thiolase domain and mediate the side-chain degradation of cholesterol; however, FadA5 and Ltp2 have been characterized as thiolase and aldolase respectively. Among them, FadA5 (steroid 3-ketoacyl-CoA thiolase) catalyses the thiolytic cleavage of 3,22-dioxyochol-4-en-24-oyl-CoA to yield 3-oxo-4-pregene-20-carboxyl-CoA and acetyl-CoA (Schaefer *et al.*, 2015). The Ltp2 catalyses the retroaldol cleavage of 17-hydroxy-3-oxo-4-pregene-20-carboxyl-CoA to yield androst-4-ene-3,17-dione and propionyl-CoA (Gilbert *et al.*, 2017). The aldolase Ltp2 associates with the hydratase ChsH2 to form the retro-aldolase complex for the side-chain degradation and the conserved domain DUF35 of ChsH2 is critical for the retroaldol activity of Ltp2 (Yuan *et al.*, 2019). A *chsH2*-like gene (*aedL*) is present in the *aed* gene cluster; the AedL belongs to the MaoC protein family and contains the DUF35 domain

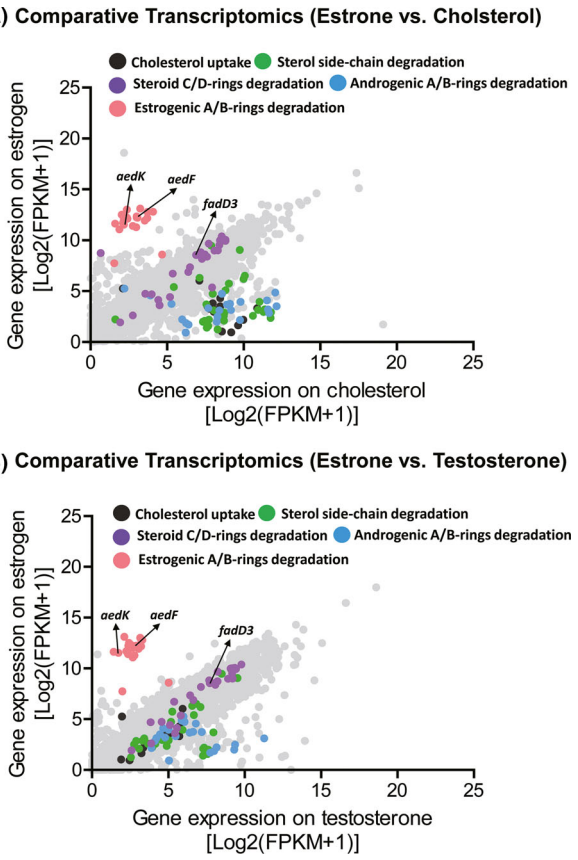

Fig. 1. Comparative transcriptomic analyses of *Rhodococcus* sp. strain B50. (A) Global gene expression profiles (RNA-Seq) of strain B50 grown on oestrone (E1) or cholesterol. (B) Global gene expression profiles of strain B50 grown on E1 or testosterone. Each spot represents a gene.

(Fig. S2). We thus speculated that AedF and AedK may participate in the thiolytic and retroaldol cleavage of the oestrogenic A/B-rings.

Functional validation of β-oxidation genes involved in oestrogen biodegradation

Next, we elucidated the function of putative thiolase and aldolase genes involved in actinobacterial oestrogen degradation. In steroid catabolic pathways, aliphatic moieties are often removed from the substrates through β-oxidation reactions, while thiolase and aldolase are critical enzymes involved in the aliphatic moiety removal (Chiang *et al.*, 2020). Thus, we disrupted two putative genes [GMFMDNLD_05335 (*aedF*) and GMFMDNLD_05342 (*aedK*)] of strain B50 through site-directed mutagenesis [insertion of a chloramphenicol-resistance gene (Cm^R) and *pheS*** cassette] (Fig. 3A). The plasmid was transferred from *Escherichia coli* (nalidixic acid-sensitive) to strain B50 (nalidixic acid-resistant) through conjugation. Subsequently, the gene-disrupted strain B50 mutants

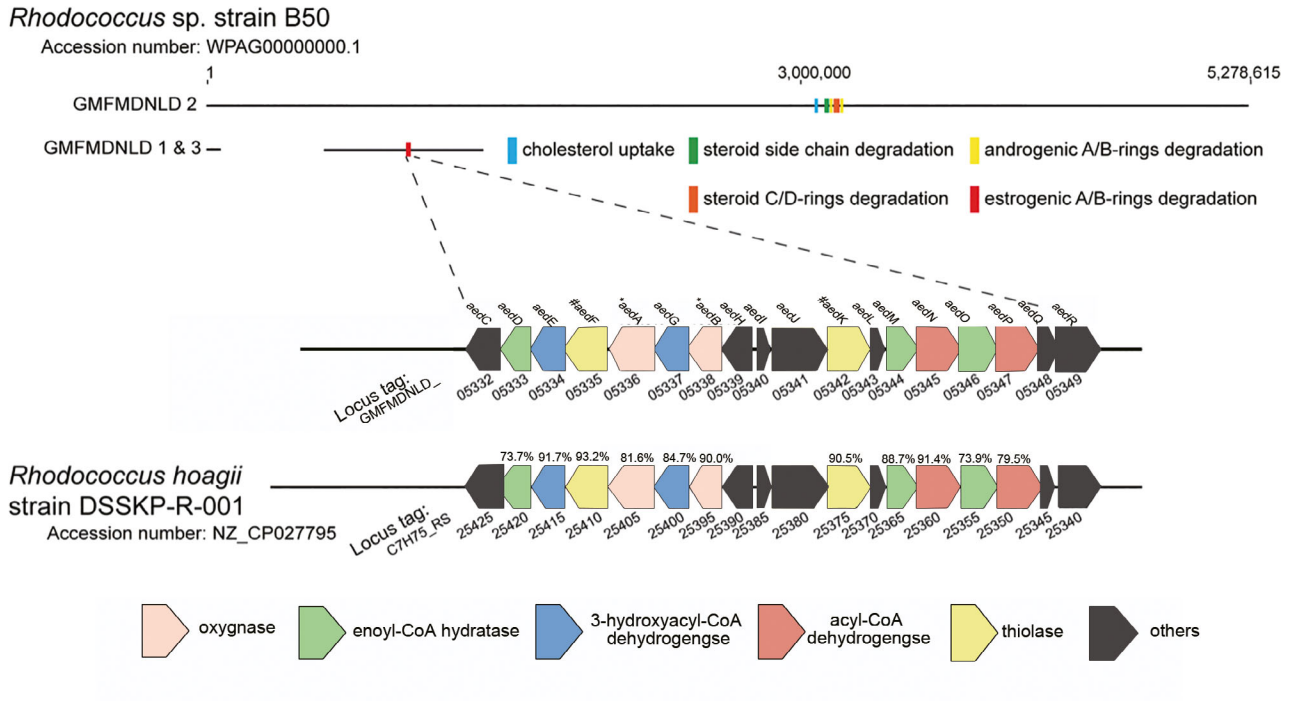

Fig. 2. The *aed* gene cluster specific for the actinobacterial degradation of oestrogenic A- and B-rings. Percentage (%) indicates the shared identity of the deduced amino acid sequences of *Rhodococcus* sp. strain DSSKP-R-001. *, the oxygenase genes *aedA* and *aed* B were characterized in our previous study (Hsiao *et al.*, 2021).

were selected and maintained on lysogeny broth (LB) agar containing two antibiotics: chloramphenicol (25 μg ml^{-1}) and nalidixic acid (12.5 μg ml^{-1}). Polymerase chain reaction (PCR) with primers flanking *aedF* and Cm^R genes confirmed the successful insertion of the chloramphenicol-resistant cassette into the *aedF* gene in the mutated strain (Fig. 3B). We then complemented the *aedF* gene (see Fig. S3A for the construct map) into the *aedF*-disrupted mutants and observed their growth patterns with E1 as the sole substrate. After the incubation with E1 for 16 h, the *aedF*-disrupted mutant culture showed a much lower increase in cell density (represented by the increase in protein concentration) (72 ± 4 μg ml^{-1}) than those of the wild-type culture (229 ± 6 μg ml^{-1}) and the complemented culture (205 ± 5 μg ml^{-1}) (Fig. 4A). The metabolite profile analysis also revealed the accumulation of a C_{17} product (**Metabolite 3**, namely 5-oxo-4-norestrogenic acid) in the E1-fed *aedF*-disrupted strain B50 mutant culture but not in the cultures of the wild-type and the complemented strain B50 (Figs 4B and 5). Applying the same gene disruption (insertion of the Cm^R and *pheS*** cassette) and complementation (see Fig. S3B for the construct map) approaches, we obtained an *aedK*-disrupted strain B50 mutant and the corresponding complemented strain (Fig. 3B). Similarly, we observed a lower increase in cell density in the *aedK*-disrupted mutant culture (105 ± 5 μg ml^{-1}) than those of the wild-type culture (225 ± 4 μg ml^{-1}) and complemented culture (214 ± 9 μg ml^{-1}) (Fig. 4A). Moreover, we detected the accumulation of a C_{15} metabolite (**Metabolite 7**, namely 2,3,4-trinorestrogenic acid) in the *aedK*-disrupted strain B50 mutant culture incubated with E1 (Figs 4B and 5).

Studies have identified 3aα-H-4α(3'-propanoate)-7aβ-methylhexahydro-1,5-indanedione (HIP) as a possible oestrogenic metabolite for proteobacteria (Wu *et al.*, 2019) and actinobacteria (Hsiao *et al.*, 2021). However, whether *fadD3* (HIP-CoA-ligase gene; GMFMDNLD_03043) is essential for oestrogen degradation remains unclear. Therefore, we disrupted *fadD3* with the Cm^R and *pheS*** cassette (Fig. 3B) and investigated E1 utilization by the wild-type strain B50, the *fadD3*-disrupted mutant and corresponding complemented strain (see Fig. S3C for the construct map). After incubation with E1 for 16 h, the *fadD3*-disrupted mutant culture showed a lower increase in cell density (141 ± 3 μg ml^{-1}) than those of the wild-type culture (232 ± 4 μg ml^{-1}) and complemented culture (221 ± 6 μg ml^{-1}) (Fig. 4A). The *fadD3*-disrupted mutant converted E1 into HIP and accumulated HIP in the culture (Fig. 4B). By contrast, the wild-type strain B50 and the complemented strain could completely degraded E1 (1 mM) within 16 h and did not accumulate HIP as an end product.

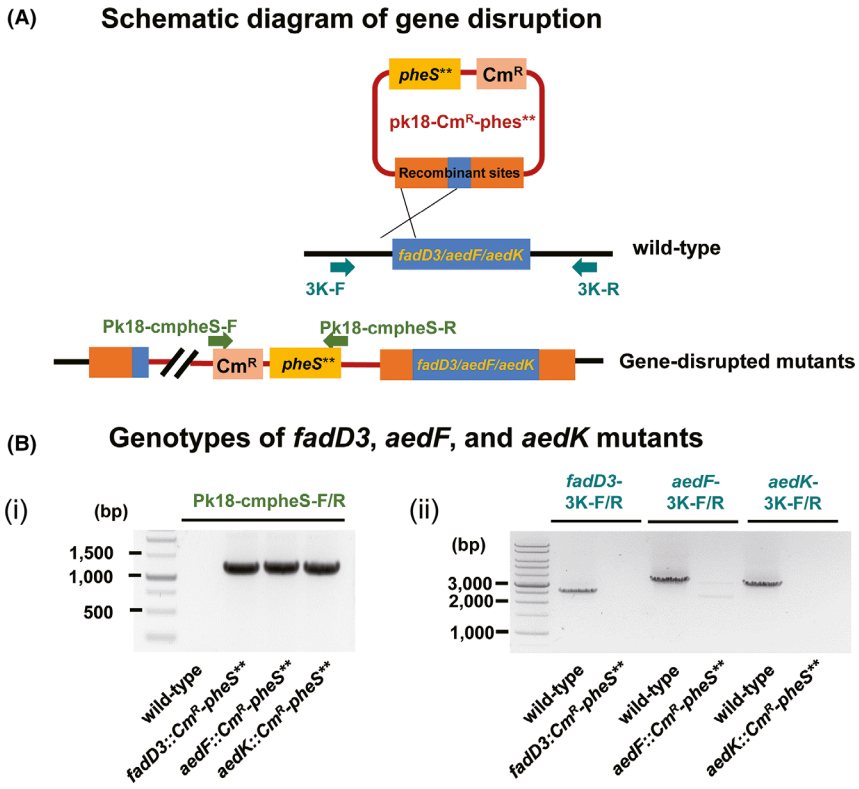

Fig. 3. Genotype examinations of strain B50 mutants. (A) Schematic of homologous recombination-mediated gene disruption. (B) Genotype examinations of gene-disrupted mutants. Agarose gel electrophoresis indicated (Bi) the insertion of a chloramphenicol-resistant gene (Cm^R) and *pheS*** cassette into target genes and (Bii) the gene disruption of strain B50 mutants. The wild-type strain B50 was also tested for comparison. (C) E1 utilization of the strain B50 mutants.

Structural elucidation of novel oestrogenic metabolites through nuclear magnetic resonance spectroscopy

We elucidated the structures of oestrogenic metabolites accumulated in the wild-type strain B50 cultures [e.g. 4-hydroxyestrone, pyridinestrone acid (PEA), Metabolite **2** and HIP] and those accumulated in the bacterial cultures of strain B50 mutants including Metabolites **3** and **7** (Table 1). Subsequently, we identified the structures of three novel oestrogen-derived metabolites through MS (Fig. S4) and NMR (see Figs S5–S10 for original NMR spectra) analyses. Among them, a high-performance liquid chromatography (HPLC)-purified compound (Metabolite **3**), obtained as a colourless oil, was assigned a molecular formula of $C_{17}H_{22}O_4$ by a quasi-molecular adduct $[M + H]^+$ at *m/z* 291.16 (calculated as 291.1596 for $C_{17}H_{23}O_4$) in the positive ion mode of ultraperformance liquid chromatography–electrospray ionization–high-resolution mass spectrometry (UPLC–ESI–HRMS; Fig. S4). When we compared the ^{1}H- and ^{13}C-NMR data of Metabolite **3** with those of the previously reported 4-norestrogenic acid (Wu *et al.*, 2019), the NMR data of Metabolite **3** were almost identical with those of 4-norestrogenic acid except that a carbonyl signal at δ_H 3.35 (H-5)/δ_C 73.8 in 4-norestrogenic acid disappeared and an additional ketone signal at δ_C 211.7 (C-5) was observed in Metabolite **3** (Table 2; see Fig. S6 for original NMR spectra), indicating that the hydroxy group at C-5 of 4-norestrogenic acid was substituted by a carbonyl in Metabolite **3**. In addition, this change was evidenced by the distinctive downfield shifts of the ^{13}C-NMR data of C-1, C-6, C-7, C-9 and C-10 of Metabolite **3**, upfield shifts of the ^{13}C-NMR data of its C-2 and C-3, and key HMBC cross-peaks of δ_H 2.55 and 2.42 (H_2-6)/δ_C 211.7 (C-5), δ_H 3.00 (H-10)/δ_C 211.7 (C-5) and δ_H 6.78 (H-1)/δ_C 211.7 (C-5) (Fig. 6; Fig. S9). The configuration of the double bond at C-1 and C-2 of Metabolite **3** was established to be an *E* form based on the larger coupling constant ($J_{H\text{-}1/H\text{-}2}$ = 15.6 Hz). Thus, the structure of Metabolite **3** was deduced and is shown in Fig. 6 – it was named 5-oxo-4-norestrogenic acid.

The NMR data of Metabolite **2** (Table 2; see Fig. S5 for original NMR spectra) were consistent with those of Metabolite **3** except an additional carbinol signal at δ_H 4.63 (H-3)/δ_C 72.8 (C-3) was observed in Metabolite **2**. Key COSY of δ_H 4.63 (H-3)/δ_H 5.56 (H-2) accompanied with key cross-peaks of δ_H 5.73 (H-1)/δ_C 72.8 (C-3), δ_H 5.56 (H-2)/δ_C 72.8 (C-3) and δ_H 5.56 (H-2)/δ_C 176.1 (C-

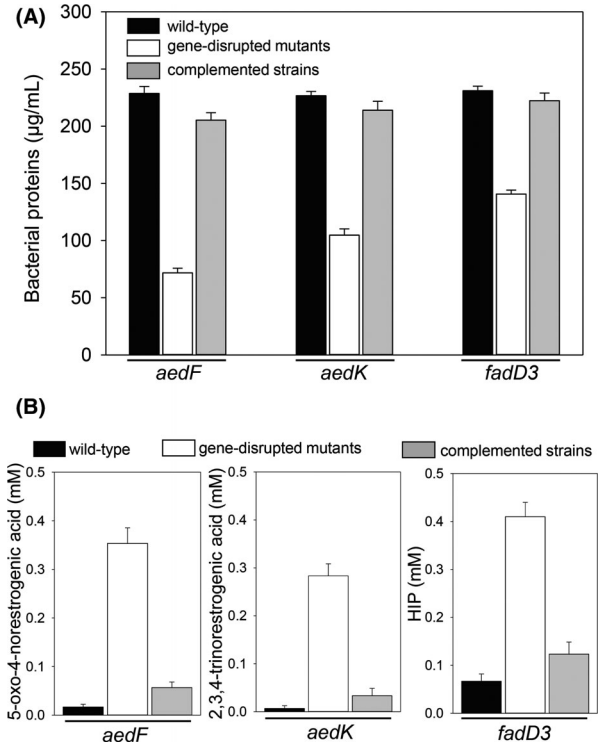

Fig. 4. Phenotype validation of the strain B50 mutants. (A) Bacterial growth (measured as the increase in total protein concentration in the E1-fed cultures) of the wild-type strain, the gene-disrupted mutants and their corresponding complemented strains. (B) The accumulation of the oestrogenic metabolites in the E1-fed cultures of the *aedF*-, *aedK*- and *fadD3*-disrupted strain B50 mutants. The cultures were incubated with E1 (1 mM) as the sole carbon source and electron donor for 16 h. The substrate was exhausted in all bacterial cultures. Total proteins and hydrophobic oestrogenic metabolites were extracted from the bacterial cultures at late log phase. The initial protein concentration in all strain B50 cultures was adjusted to 50 ± 4 μg ml^{-1}. Data shown are the means ± SD from three experimental measurements.

4) in the HMBC spectrum (Fig. 6; Fig. S8) confirmed the additional carbinol was attached at C-3. The assignments matched with the molecular formula of compound **2**, $C_{18}H_{24}O_5$, as interpreted from a quasi-molecular adduct $[M + H]^+$ at *m/z* 321.17 (calculated as 321.1702 for $C_{18}H_{25}O_5$) in the positive ion mode of UPLC–ESI–HRMS (Fig. S4). The configuration of the double bond at C-1 and C-2 of Metabolite **2** was established to be an *E* form based on the larger coupling constant ($J_{H\text{-}1/H\text{-}2}$ = 16.2 Hz). The structure of Metabolite **2** is shown in Fig. 6, and it was named 4,5-*seco*-estrogenic acid.

The NMR data of Metabolite **7** (Table 2; see Fig. S7 for original NMR spectra) coincided well with those of Metabolite **3** except the notable upfield shifts of C-8 and C-9 of Metabolite **7**, indicating conspicuous changes on the B-ring of Metabolite **7**. Key COSY of δ_H 2.33 (H_2-6)/δH 1.82 (H_2-7) and δ_H 1.60 (H-9)/δ_H 2.13 and 2.60 (H_2-10) together with key cross-peaks of δ_H 2.33 (H_2-6)/δ_C 177.8 (C-5), δ_H 2.33 (H_2-6)/δ_C 39.9 (C-8), δ_H 1.82 (H_2-7)/δ_C 177.8 (C-5), δ_H 1.60 (H-9)/δ_C 177.1 (C-1) and δ_H 2.13 and 2.60 (H_2-10)/δ_C 177.1 (C-1) in the HMBC spectrum (Fig. 6; Fig. S10) corroborated that the B-ring of Metabolite **7** was opened and with two terminal carboxylic acids at C-1 and C-5. After being further confirmed by a quasi-molecular adduct $[M + H]^+$ at *m/z* 283.15 (calculated as 283.1545 for $C_{15}H_{23}O_5$) from the UPLC–ESI–HRMS data analysis (Fig. S4), the structure of Metabolite **7** was elucidated, as shown in Fig. 6, and it was named 2,3,4-trinorestrogenic acid.

UPLC–ESI–HRMS detection of CoA-ester intermediates involved in the actinobacterial degradation of oestrogen A/B-rings

We then managed to identify the hypothetical CoA-ester intermediates. The wild-type strain B50 and the *aed*-disrupted mutants were incubated with E1 in the same chemically defined mineral medium abovementioned. After the substrate was apparently consumed, strain B50 cells were harvested through centrifugation and then lysed through sonication. After partial purification via the solid-phase extraction (C_{18}), the CoA-ester extracts were subject to UPLC–ESI–HRMS analysis in positive mode. We observed an $[M + H]^+$ adduct (*m/z* = 1040.27; retention time = 4.03 min) corresponding to the monoisotopic mass of the CoA-ester form of **Metabolite 3** in the CoA-ester extracts of the *aedF*-disrupted mutant (Fig. 7C). Moreover, the characteristic fragment adduct of CoA (*m/z* = 768.12) (Wu *et al*., 2019) is also present in the MS spectrum of this compound. We also detected an $[M + H]^+$ adduct (*m/z* = 1032.26; retention time = 4.22 min) corresponding to the monoisotopic mass of the CoA-ester form of **Metabolite 7** in the CoA-ester extracts of the *aedK*-disrupted mutant (Fig. 7D). The adducts corresponding to the two CoA-esters were not detected in the wild-type strain B50 cultures.

Discussion

Establishment of an oestrogen degradation pathway in actinobacteria

In a previous study, we identified initial metabolites (namely 4-hydroxyestrone and PEA) along with two oxygenase genes (namely *aedA* and *aedB*) in strain B50 (Hsiao *et al*., 2021). Moreover, the findings of comparative genomic analysis indicated that this *aed* gene cluster is present in some oestrogen-degrading *Rhodococcus* strains, including the oestrogen-degrading *R. equi* DSSKP-R-001 (Zhao *et al*., 2018; Tian *et al*., 2020). Furthermore, the transcriptome analysis showed that > 720 genes, including many *aed* genes, were significantly up-regulated in the oestrogens-treated strain DSSKP-R-001

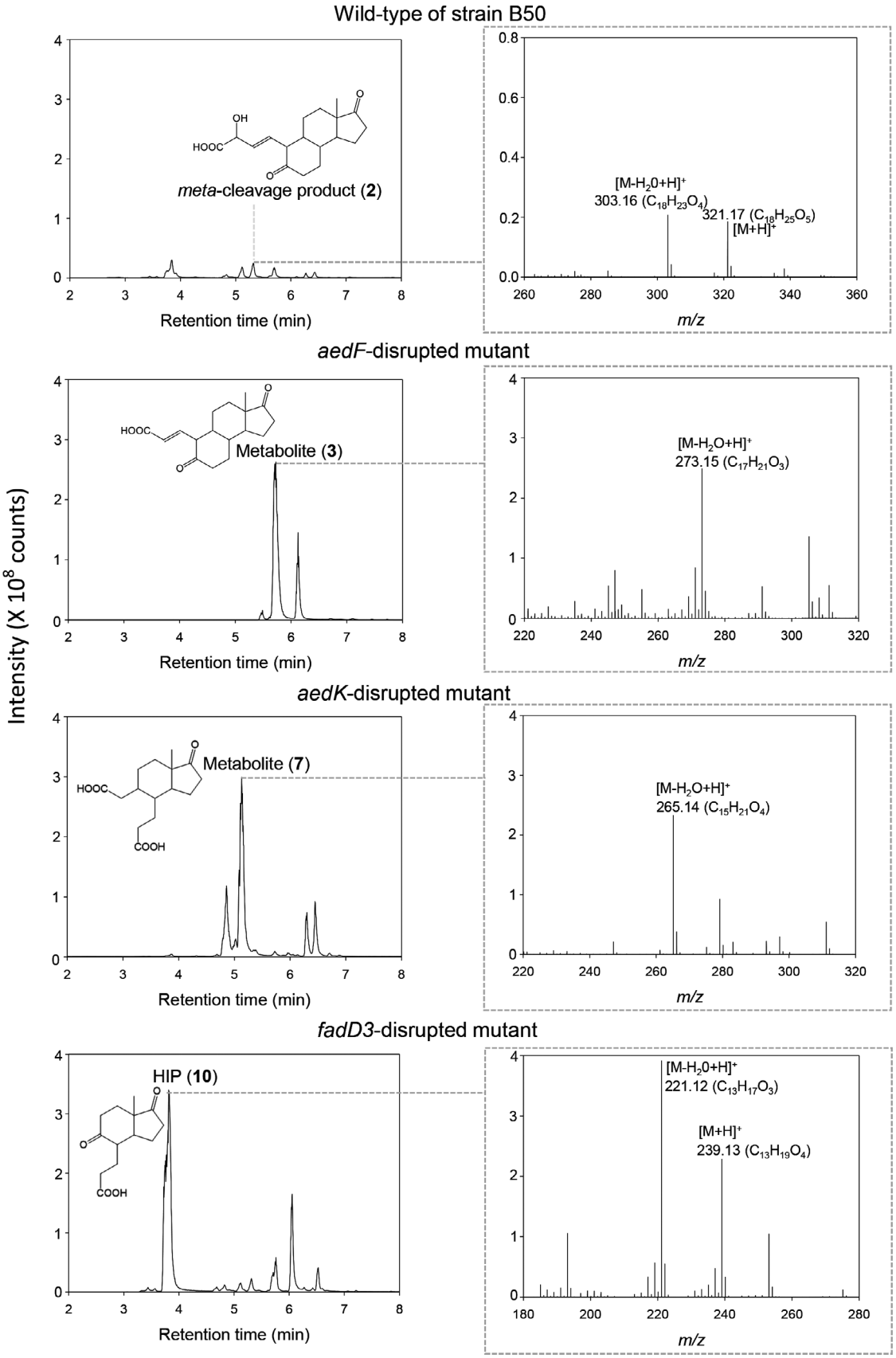

Fig. 5. UPLC−APCI−HRMS identification of C_{17} (Metabolite **3**, namely 5-oxo-4-norestrogenic acid), C_{15} (Metabolite **7**, namely 2,3,4-trinorestrogenic acid) and C_{13} (HIP) metabolites in the E1-fed cultures of *aedF*-, *aedK*- and *fadD3*-disrupted mutants respectively. The major oestrogenic metabolites observed in the wild-type strain B50 culture include the C_{18} *meta*-cleavage product (Metabolite **2**).

Table 1. UPLC-HRMS analysis of metabolites involved in oestrogen degradation by strain B50. Oestrogenic metabolites newly identified in this study are boldfaced.

Compound ID	UPLC behaviour (RT[a], min)	Molecular formula/ (predicted molecular mass)[b]	Dominant ion peaks	Identification of product ions	Mode observed
E1	8.13	$C_{18}H_{22}O_2$	253.16	$[M\text{-}H_2O+H]^+$	ESI and APCI
		270.16	271.17	$[M + H]^+$	ESI and APCI
4-hydroxyestrone	7.40	$C_{18}H_{22}O_3$	269.16	$[M\text{-}H_2O+H]^+$	APCI
		286.16	287.15	$[M + H]^+$	ESI and APCI
			309.15	$[M+Na]^+$	ESI
PEA*	4.02	$C_{18}H_{21}O_3N$	282.17	$[M\text{-}H_2O+H]^+$	ESI
		299.15	300.16	$[M + H]^+$	ESI and APCI
			322.15	$[M+Na]^+$	ESI
4,5-*seco*-estrogenic acid (Metabolite **2)**	5.24	$C_{18}H_{24}O_5$	303.16	$[M\text{-}H_2O+H]^+$	ESI and APCI
		320.17	321.17	$[M + H]^+$	ESI and APCI
			343.15	$[M+Na]^+$	ESI
5-oxo-4-norestrogenic acid (Metabolite **3)**	5.82	$C_{17}H_{22}O_4$	273.15	$[M\text{-}H_2O+H]^+$	ESI and APCI
		290.16	291.16	$[M + H]^+$	ESI and APCI
			313.14	$[M+Na]^+$	ESI
2,3,4-trinorestrogenic acid (Metabolite **7)**	5.08	$C_{15}H_{22}O_5$	247.13	$[M\text{-}2H_2O+H]^+$	ESI and APCI
		282.15	265.14	$[M\text{-}H_2O+H]^+$	ESI and APCI
			283.15	$[M + H]^+$	ESI and APCI
HIP	3.81	$C_{13}H_{18}O_4$	221.12	$[M\text{-}H_2O+H]^+$	ESI and APCI
		238.12	239.13	$[M + H]^+$	ESI and APCI
			261.11	$[M+Na]^+$	ESI

a. RT, retention time.
b. The predicated molecular mass was calculated using the atom masses of ^{12}C (12.00), ^{16}O (15.99) and ^{1}H (1.01).
*. PEA is a dead-end product.

cells (Tian *et al.*, 2020). Interestingly, the *aed* gene cluster is also located on the plasmid (plas2; 95 132 bp) of the strain DSSKP-R-001. In both strains (B50 and DSSKP-R-001), the *aed* gene cluster is flanked by transposon elements and transposases, suggesting that the *aed* genes are likely horizontally transferred between actinobacteria.

Transcriptomic analyses require active cells with mRNA of high quality. Therefore, we cultivated the wild-type strain B50 with different steroid substrates and harvested the bacterial cells at the mid-log phase (OD_{600} = 0.4~0.5). By contrast, we used the resting cells of the wild-type strain B50 or the gene-disrupted mutants to accumulate oestrogenic metabolites. Since resting cells halt anabolism and only catabolize substrates, it is easier to observe a simplified metabolite profile with sequential production of metabolites in sufficient quantity and on a shorter timeline. In the present study, the findings of comparative transcriptomic analysis demonstrated that *aed* genes are differentially induced by E1 but not by testosterone or cholesterol. Subsequently, we demonstrated the essential role of three genes involved in the β-oxidation of oestrogenic A/B-rings including *aedF*, *aedK* and *fadD3*. These mutants enabled the accumulation of new oestrogenic metabolites in bacterial cultures. Together, an oestrogen degradation pathway in actinobacteria was established (Fig. 8). The complete set of the oestrogenic metabolite profile and the degradation genes of both actinobacteria and proteobacteria may allow for the facile monitoring of oestrogen biodegradation in various ecosystems through liquid chromatography–mass spectrometry analysis and PCR-based functional assays.

Identification of essential β-oxidation genes and corresponding metabolites for oestrogen degradation enabled the establishment of a complete degradation pathway in actinobacteria. Briefly, in the proposed pathway, the C-4 of E1 is first hydroxylated by oestrone 4-hydroxylase AedA, and the resulting catecholic A-ring is cleaved through *meta*-cleavage by 4-hydroxyestrone 4,5-dioxygenase AedB. In the presence of ammonium, the *meta*-cleavage product may undergo abiotic recyclization to produce the nitrogen-containing metabolite PEA (Hsiao *et al.*, 2021). In addition, the dead-end product PEA was detected during oestrogen degradation by proteobacteria (Chen *et al.*, 2018; Ibero *et al.*, 2019a,b; 2020). In proteobacteria, only a minor part (approximately 2%) of the *meta*-cleavage product is abiotically transformed into PEA (Wu *et al.*, 2019). Actinobacteria

Table 2. ^{1}H- (600 MHz) and ^{13}C-NMR (150 MHz) spectral data of 5-oxo-4-norestrogenic acid (Metabolite **3**), 4,5-*seco*-estrogenic acid (Metabolite **2**) and 2,3,4-trinorestrogenic acid (Metabolite **7**).

	Metabolite 3		Metabolite 2		Metabolite 7	
Positions	^{1}H[a,b]	^{13}C[a]	^{1}H[a,b]	^{13}C[a]	^{1}H[a,b]	^{13}C[a]
1	6.78 dd (9.6, 15.6)	147.1	5.73 dd (10.2, 16.2)	131.5		177.1
2	5.79 d (15.6)	126.2	5.56 dd (6.3, 16.2)	132.5		
3		169.4	4.63 d (6.3)	72.8		
4				176.1		
5		211.7		213.3		177.8
6	2.55 m	42.2	2.54 m	42.3	2.33 m	30.5
	2.42 m		2.41 m			
7	2.20 m	31.5	2.18 m	31.7	1.82 m	25.3
	1.44 m		1.43 m			
8	1.90 m	40.4	1.83 m	40.6	1.60 [d]	39.9
9	1.41 m	49.9	1.28 m	50.5	1.60 [d]	39.2
10	3.18 t (10.2)	59.9	3.00 t (10.2)	60.2	2.60 m	39.0
					2.13 [c]	
11	1.60 m	28.7	1.73 m	28.6	1.76 m	29.0
	1.40 m		1.34 m		1.48 m	
12	1.75 m	32.3	1.72 m	32.4	1.69 m	32.6
	1.28 m		1.26 m		1.28 m	
13		49.4		49.5		49.5
14	1.47 m	51.2	1.42 m	51.4	1.53 m	50.0
15	2.02 m	22.8	2.04 m	22.8	2.02 m	23.5
	1.67 m		1.70 m		1.69 m	
16	2.48 dd (8.4, 19.2)	36.7	2.48 dd (8.4, 19.2)	36.8	2.46 dd (9.0, 19.2)	36.7
	2.13 dd (9.6, 19.2)		2.10 dd (9.0, 19.2)		2.13 [c]	
17		223.1		223.3		223.7
18	0.98 s	14.4	0.98 s	14.5	0.90 s	14.1

[a]Measured in methanol-d_4. [b] δ in ppm, mult. (J in Hz). [c,d]Signals were overlapped and picked up from HMBC or HSQC experiments. The original NMR spectra of Metabolites **2**, **3** and **7** are shown in Figs S2–S4 respectively.

produced even less PEA (< 0.5%) during E1 degradation (Hsiao *et al*., 2021), suggesting that the most *meta*-cleavage product was further degraded.

Biochemical mechanisms and corresponding genes involved in oestrogenic A- and B-rings degradation

Subsequent reactions may include the formation of CoA-esters through putative CoA-ligase (*aedJ*; GMFMDNLD_05341), followed by the AedF-mediated removal of the C-2 and C-3 of CoA-esters through the first cycle of thiolytic β-oxidation. A highlight of the present study is the identification of two novel CoA-esters from the *aed*-disrupted strain B50 cultures (Fig. 7). Similar procedure has been applied to extract and to identify a CoA-ester [4-norestrogen-5(10)-en-3-oyl-CoA] of the proteobacterial *Sphingomonas* sp. strain KC8, indicating that the method combining solid-phase extraction and UPLC–ESI–HRMS are suitable for analysing CoA-ester metabolites derived from oestrogens. We could not detect the CoA-esters (metabolites 5 to 12) in the wild-type strain B50 cultures. This is likely due to that metabolic pathway in the wild-type strain B50 cells is not blocked. Nonetheless, the detection of E1-derived CoA-esters in the strain B50 mutants supported our hypothesis that CoA-esters, but not the deconjugated structures, are the intermediates in the actinobacterial oestrogen degradation pathway. CoA is an essential cofactor in numerous biosynthetic and energy-yielding metabolic pathways. When CoA is required in other metabolic pathways, CoA-esters in the steroid degradation pathways can be deconjugated (Takamura and Nomura, 1988; Lin *et al*., 2015; Wu *et al*., 2019). The disruption of thiolase genes thus resulted in the production and excretion of deconjugated metabolites such as **Metabolites 3** and **7** in E1-fed cultures. We failed to purify and characterize other oestrogenic metabolites (e.g. **Metabolites 5** and **9**) from bacterial extracts partially because (i) these compounds are chemically unstable, or (ii) these compounds are toxic to bacteria and are accumulated in cells in trace amounts.

Thus far, the mechanism operating in the actinobacterial oestrogenic B-ring cleavage remains unclear. Proteobacteria degrade the oestrogenic B-ring through hydrolysis (Wu *et al*., 2019; Ibero *et al*., 2020), and a similar hydrolytic ring cleavage mechanism has been demonstrated in the degradation of cyclohexanecarboxylic acid by the alphaproteobacterium *Rhodopseudomonas palustris* (Pelletier and Harwood, 1998, 2000). Therefore, the oestrogenic B-ring is likely cleaved by strain B50 through a similar hydrolytic cleavage. However, a *badI*-like gene has not been identified in the

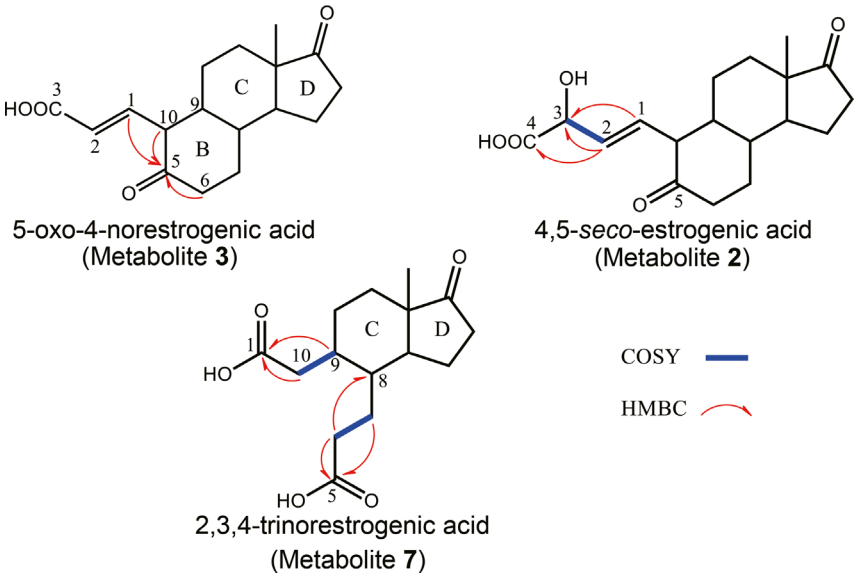

Fig. 6. Key COSY and HMBC correlations in the two-dimensional NMR data of three HPLC-purified metabolites produced by strain B50. Original COSY and HMBC spectra of Metabolites **2**, **3** and **7** are provided in Figs S8, S9 and S10 respectively

strain B50 genome, likely due to a low sequence similarity between actinobacterial and proteobacterial genes.

Another highlight of the present study is the NMR identification of a C_{15} oestrogenic metabolite 2,3,4-trinorestrogenic acid from *aedK*-disrupted strain B50 cultures, which validated the function of *aedK* and the proposed catabolic pathway involved in oestrogenic B-ring degradation. After the hydrolytic cleavage of the oestrogenic B-ring, the AedK-mediated removal of C-1 and C-10 at the CoA-ester of Metabolite **7** through the second cycle of aldolytic β-oxidation yielded HIP (Fig. 8). In the linear chromosome of strain B50, we identified a typical gene cluster specific for actinobacterial HIP degradation (Bergstrand *et al.*, 2016; Crowe *et al.*, 2018). The disruption of *fadD3* resulted in apparent HIP accumulation in E1-fed strain B50 cultures, indicating the essential role of this gene cluster in oestrogenic C- and D-rings degradation.

Activation mechanisms of the meta-cleavage product likely differ between actinobacteria and proteobacteria

Using strain B50 and *Sphingomonas* sp. strain KC8 as the model actinobacterium and proteobacterium, respectively, our data revealed that the actinobacterial oestrogen degradation pathway is highly similar to the proteobacterial pathway (Fig. 8; Chen *et al.*, 2017; Wu *et al.*, 2019; Ibero *et al.*, 2020); however, their metabolite profiles appear to be distinguishable. For example, oestrogenic metabolites from actinobacteria have a typical 5-oxo group, whereas oestrogenic metabolites in proteobacteria have a typical hydroxyl group at their C-5. Moreover, actinobacteria and proteobacteria seem to employ different biochemical mechanisms for oestrogenic A-ring cleavage. The A-ring-cleaved metabolite in strain KC8 possesses three unsaturated double bonds at C-1, C-3 and C-5, which readily undergoes abiotic recyclization to produce PEA in the presence of ammonium, whereas strain B50 adopts an extradiol dioxygenase AedB to produce 4,5-*seco*-estrogenic acid, which has only two double bonds at C-1 and C-5 and is less likely recyclized.

Actinobacteria and proteobacteria appear to adopt different strategies to oxidize the A-ring-cleaved product (Fig. 8). *Sphingomonas* sp. strain KC8 depends on the 2-oxoacid oxidoreductase EdcC, a member of the indolepyruvate ferredoxin oxidoreductase family, to produce 4-norestrogen-5(10)-en-3-oyl-CoA through a single oxidative decarboxylation step (Wu *et al.*, 2019; Ibero *et al.*, 2020). The homologous 2-oxoacid oxidoreductase gene was absent in the genome of strain B50 and any other oestrogen-degrading actinobacteria. In strain B50, a putative 2-hydroxyacid dehydrogenase gene (GMFMDNLD_05337; *aedG*), a decarboxylase gene (GMFMDNLD_05339; *aedH*) and a CoA-ligase gene (GMFMDNLD_05341; *aedJ*) on the megaplasmid likely serve to add a CoA onto 4,5-*seco*-estrogenic acid (namely Metabolite **2**) through three different steps. Nevertheless, the functions of these genes remain to be characterized.

Experimental procedures

Chemicals

Cholesterol, E1, E2, E3, 4-hydroxyestrone, 17α-ethynylestradiol, HIP [also known as 3-(7a-methyl-1,5-

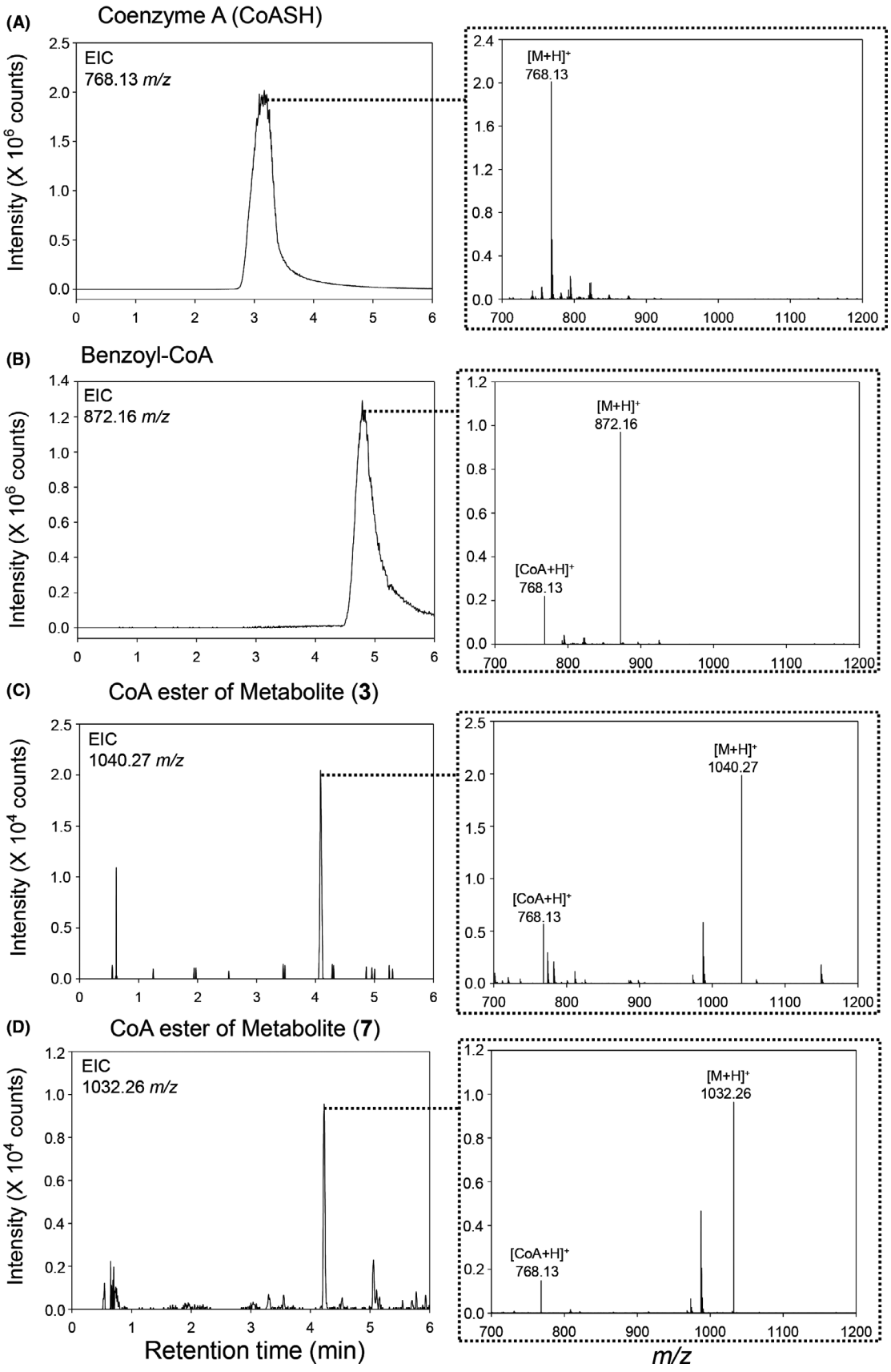

Fig. 7. Extracted ion chromatograms (EIC) and MS spectra of two authentic standards, CoA-SH (A) and benzoyl-CoA (B), and the E1-derived CoA-esters of Metabolite **3** (C) and Metabolite **7** (D). The wild-type of strain B50 was incubated with E1 (1 mM), and the CoA-esters were extracted from the cell lysate through solid-phase extraction. The fragment ion (*m/z* = 768.13) peak corresponding to the CoA moiety was observed in the MS spectra of benzoyl-CoA and the CoA-ester of Metabolites **3** and **7**.

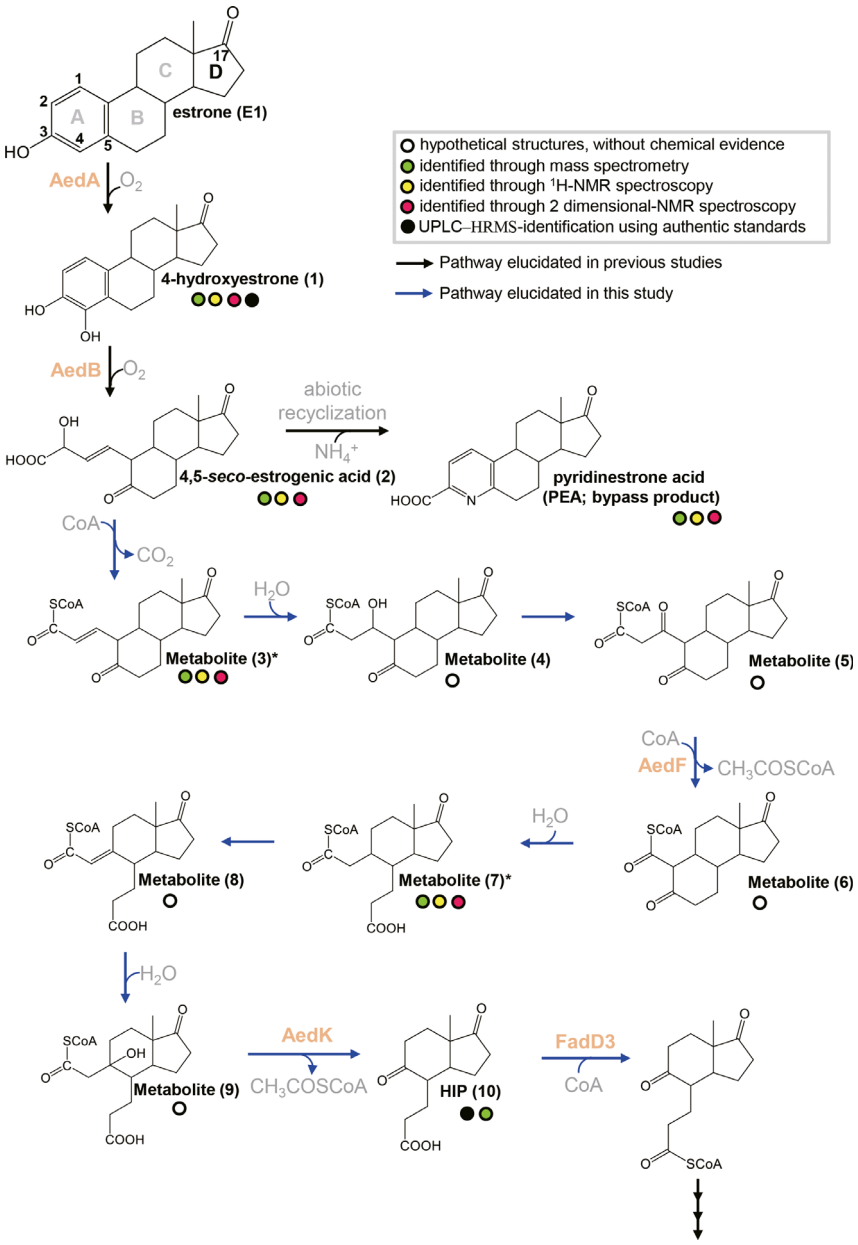

Fig. 8. The proposed oestrogen degradation pathway of actinobacteria. *, the deconjugated structures have been purified and elucidated in this study. *AedF*, *AedK* and *fadD3* have been functionally characterized in the study.

dioxooctahydro-1H-inden-4-yl) propanoic acid] and testosterone were purchased from Sigma-Aldrich (St. Louis, Missouri, USA). PEA was prepared as described by Chen *et al.*, 2017. The [3,4C-^{13}C]E1 (99%) was purchased from Cambridge Isotope Laboratories (Tewksbury, Massachusetts, USA). All other chemicals were of analytical grade and purchased from Honeywell Fluka (Loughborough, UK), Mallinckrodt Baker (Phillipsburg, NJ, USA), Merck (Darmstadt, Germany) and Sigma-Aldrich.

Aerobic incubation of strain B50 with sex steroids

The wild-type and the gene-disrupted mutants of strain B50 were used in resting cell biotransformation assays. Bacteria were first aerobically grown in LB broth (1 l in a 2-l Erlenmeyer flask) containing E1 (50 μM) as an inducer at 30°C with continuous shaking (150 rpm). Cells were collected through centrifugation (8000 *g*, 20 min, 15 °C). The cell pellet was resuspended in a chemically defined mineral medium contained NH_4Cl (2.0 g l^{-1}), KH_2PO_4 (0.67 g l^{-1}), K_2HPO_4 (3.95 g l^{-1}), $MgSO_4$ (2 mM), $CaCl_2$ (0.7 mM), filtered vitamin mixture (as described in DSMZ 1116 medium), ethylenediaminetetraacetic acid (EDTA)-chelated mixture of trace elements (Rabus and Widdel, 1995) and sodium selenite (4 μg l^{-1}). The cell suspension (OD_{600} = 1; 1 l) was incubated with E1 or other sex steroids (1 mM) and was aerobically incubated at 30 °C with continuous shaking (150 rpm) for 24 h. A remarkable characteristic of steroids is their extremely low aqueous solubility (< 20 mg l^{-1}) (Chiang *et al.*, 2020). Thus, 8 ml of the stock solution containing 125 mM steroid substrate (E1 or other steroids) dissolved in dimethyl sulphoxide (DMSO) was added to the bacterial cultures (1 l); the final DMSO content was 0.8% (v/v). After aerobic incubation with steroid substrates for 16 h, the resulting samples were acidified using 6N HCl and extracted twice by using equal volumes of ethyl acetate. Ethyl acetate fractions were evaporated, and pellets containing oestrogenic metabolites were stored at −20 °C until further analysis.

HPLC

A reversed-phase HPLC system (Hitachi, Tokyo, Japan) was used for the separation of oestrogenic metabolites. Separation was achieved on an analytical RP-C_{18} column [Luna C_{18}(2), 5 μm, 150 × 4.6 mm; Phenomenex, Torrance, CA, USA] with a flow rate of 0.8 ml min^{-1}. Separation was isocratically performed with 30% (vol/vol) acetonitrile containing formic acid (0.1%; vol/vol) serving as the eluent. Steroid products were detected in the range of 200–450 nm by using a photodiode array detector.

Solid-phase extraction

HPLC-purified samples were further concentrated through solid-phase extraction (SPE). The 1-ml BAKERBOND™ SPE Octadecyl (C_{18}) Disposable Extraction Columns (J.T. Baker, Avantor, Radnor, PA, USA) was preconditioned with 1 ml of methanol and 1 ml of ddH_2O (pH 2). Samples were evaporated for 30 min to eliminate acetonitrile before loading onto SPE cartridges. Samples were eluted with 1.5 ml of methanol. The eluate was evaporated for further UPLC–HRMS and NMR analysis.

UPLC–APCI–HRMS

Ethyl acetate extractable samples or HPLC-purified oestrogenic metabolites were analysed on an UPLC system coupled to an APCI–mass spectrometer. Separation was achieved on a reversed-phase C_{18} column (Acquity UPLC® BEH C_{18}; 1.7 μm; 100 × 2.1 mm; Waters, Milford, Massachusetts, USA) with a flow rate of 0.4 ml min^{-1} at 50 °C (column oven temperature). The mobile phase comprised a mixture of two solvents: Solvent A [2% (vol/vol) acetonitrile containing 0.1% (vol/vol) formic acid] and Solvent B [methanol containing 0.1% (vol/vol) formic acid]. Separation was achieved using a linear gradient of Solvent B from 5% to 99% across 12 min. Mass spectrum data were obtained using a Thermo Fisher Scientific Orbitrap Elite Hybrid Ion Trap-Orbitrap Mass Spectrometer (Waltham, MA, USA) equipped with a standard APCI source operating in the positive ion mode. In APCI–HRMS analysis, the capillary and APCI vaporizer temperatures were 120 °C and 400 °C, respectively; the sheath, auxiliary and sweep gas flow rates were 40, 5 and 2 arbitrary units respectively. The source voltage was 6 kV, and the current was 15 μA. The parent scan was in the range of *m/z* 50–600. The predicted elemental composition of individual intermediates was calculated using Xcalibur™ Software Mass Spectrometry Software (Thermo Fisher Scientific, Waltham, MA, USA).

UPLC–ESI–HRMS

HPLC-purified oestrogenic metabolites were also analysed through UPLC–ESI–HRMS on a UPLC system coupled to an ESI–mass spectrometer. UPLC separation was achieved as described above. Mass spectral data were collected in a +ESI mode in separate runs on a Thermo Fisher Scientific Orbitrap Elite Hybrid Ion Trap-Orbitrap Mass Spectrometer (Waltham, MA, USA) operated in a scan mode of 50–500 *m/z*. The source voltage was set at 3.2 kV; the capillary and source heater temperatures were 360 °C and 350 °C, respectively; the sheath, auxiliary and sweep gas flow rates were 30, 15 and 2 arbitrary units respectively. The predicted elemental composition of individual intermediates was calculated using Xcalibur™ Software Mass Spectrometry Software (Thermo Fisher Scientific).

NMR spectroscopy

^1H-, ^{13}C- and two-dimensional NMR spectra including COSY, HSQC and HMBC were recorded at 298°K by using an Agilent 600 MHz DD2 spectrometer (Agilent, Santa Clara, CA, USA). Chemical shifts (δ) were recorded and presented in parts per million with

deuterated methanol (99.8%) as the solvent and internal reference.

PCR

Bacterial genomic DNA (gDNA) was extracted using the Presto Mini gDNA Bacteria Kit (Geneaid, New Taipei City, Taiwan). DNA fragments used for plasmid assembly were amplified with Platinum polymerase (Thermo Fisher Scientific), and PCR products were purified using the GenepHlow Gel/PCR Kit (Geneaid, New Taipei City, Taiwan). For colony PCR reactions, a single colony of strain B50 was dissolved in 50 μl of InstaGene™ Matrix (Bio-Rad, Hercules, CA, USA). Strain B50 cell lysate (5 μl) was added into the PCR mixture (25 μl) containing nuclease-free H_2O, 2× PCR buffer (12.5 μl), dNTPs (0.4 mM), *Taq* polymerase (2.5 U), Red dye and PCR stabilizer (TOOLS, Taipei, Taiwan), and forward and reverse primers (each 400 nM). PCR products were visualized using standard TAE-agarose gel (1%) electrophoresis with SYBR Green I nucleic acid gel stain (Thermo Fisher Scientific).

The fadD3, aedF and aedK disruption in strain B50

The disruption of individual thiolase genes (*aedF* or *aedF*) or *fadD3* in strain B50 was performed using homologous recombination by a pK18-Cm^R-pheS** plasmid, as described previously (Hsiao *et al.*, 2021). Briefly, recombinant sites including the 900 base pair upstream/downstream flanking region and the 100 base pair coding sequence of the target genes were cloned into pK18-Cm^R-pheS** plasmid backbone by using an In-Fusion® HD Cloning Kit (TAKARA Bio; Kusatsu, Shiga, Japan) to generate the plasmid (*aedF*-, *aedK*- or *fadD3*-pK18-Cm^R-pheS**). This plasmid was electroporated into *E. coli* strain S17-1 using a Gene Pulser Xcell™ (Bio-Rad, Hercules, CA, USA) with the conditions of 2.5kV, 25μF and 200Ω. The transformed *E. coli* strain S17-1 was co-incubated with wild-type *Rhodococcus* sp. strain B50 at 30 °C overnight for horizontal gene transfer through conjugation. Successfully transformed colonies of *Rhodococcus* sp. strain B50 were selected with nalidixic acid and chloramphenicol. The insertion of the chloramphenicol-resistant gene into the strain B50 genome was confirmed using the plasmid-specific primer pairs 5′-TTCATCATGCCGTTTGTGAT- 3′ (Pk18-cmpheS-F) and 5′- ATCGTCAGACCCTTGTCCAC- 3′ (Pk18-cmpheS-R). The genotypes of the *aedF*-, *aedK*- and *fadD3*-disrupted mutants were examined using the gene-specific primer pairs: 5′-GCGTCACCCGGATCTGAAGA-3′ (*aedF*-3k-F) and 5′- GTCGGTTGAATTGGACGAGTGTG-3′ (*aedF*-3k-R), 5′-CCGCGAAACATCTTCCTC-3′ (*aedK*-3k-F) and 5′-CCGCCGCCATCCCGTAGG-3′ (*aedK*-3k-R), and 5′-GATTCTCTTCGAGCCACTGC-3′ (*fadD3*-3k-F) and 5′-GCAGATCCACTACTTCGCTC-3′ (*fadD3*-3k-R) respectively (Table S1).

Complementation of fadD3, aedF and aedK in the gene-disrupted mutants

To construct mutants for complementation and E1 utilization experiments, the PCR-amplified *fadD3*, *aedF* or *aedK* was inserted into the plasmid pMNMCSK by using an In-Fusion® HD Cloning Kit to construct *fadD3*-pMNMCSK, *aedF*-pMNMCSK and *aedK*-pMNMCSK respectively (see Fig. S3 for their construct map). The resulting plasmids were maintained in *Escherichia coli* strain DH5α and provided apramycin (50 μg ml^{-1}) resistance for the host cells. The complementation constructs *fadD3*-pMNMCSK, *aedF*-pMNMCSK and *aedK*-pMNMCSK were respectively transformed into the *fadD3*, *aedF* and *aedK*-disrupted mutants through electroporation (2.5 kV, 25 μF and 200 Ω); the complementation strains (with chloramphenicol and apramycin resistance) of strain B50 were selected. Retention of the plasmids in the transformants was confirmed through PCR using the pMNMCSK vector-specific primer pairs: 5'- CTCACTGCACGGAGGAAC- 3' (pMNMCSK-seq-F) and 5'- CGAGTCAGTGAGCGAGG- 3' (pMNMCSK-seq-R). The oestrogen utilization capacity of these B50 mutants was investigated by determining the total proteins in the E1 (1 mM)-fed bacterial cultures. The wild-type of strain B50 was used for a comparison.

Measurement of protein content

Culture samples (1 ml) were centrifuged at 10 000 *g* for 5 min. After centrifugation, the pellet was resuspended in 100 μl of extraction reagent (BugBuster® Master Mix, Merck Millipore, MA, USA) contained protease inhibitor and then incubated at room temperature for 30 min. The cell lysates were then centrifuged at 20 000 *g* for 20 min at 4 °C to remove the cell debris. The protein content of the supernatant was determined using a BCA assay (Pierce™ BCA protein assay kit; Thermo Fisher Scientific) according to manufacturer's instructions with bovine serum albumin as the standard.

Extraction and identification of CoA-ester intermediates derived from E1

The resting cells of the wild-type strain B50 as well as the *aedF*- and *aedK*-disrupted mutants were prepared as described above and incubated with E1 for 16 h. The E1-fed strain B50 cells were harvested by centrifugation and stored at −80 °C. The frozen cells were gently resuspended in 0.6 ml of double distilled water and then

cells were disrupted through sonication (Bioruptor® Pico Sonication System, Diagenode, Denville, NJ, USA) at 4 °C for 20 min (20 cycles of 30 s on/30 s off). After sonication, 30 μl of 6N HCl was added to the cell lysate, vortexed for 5 min and centrifuged at 13 500 *g* for 5 min. The CoA-esters were extracted through solid-phase extraction [Bakerbond™ SPE Octadecyl (C18) Disposable Extraction Column (1 ml) with 100 mg of sorbent] as described (27, 29) with minor modifications. The attached CoA-esters were eluted with 1 ml of 30% aqueous methanol (vol/vol) and subjected to UPLC–ESI–HRMS analysis. Two reference compounds, CoA-SH and benzoyl-CoA, were used to confirm the extraction efficiency of the solid-phase extraction method. The mobile phase for the UPLC separation comprised a mixture of two solvents: Solvent A [2% (vol/vol) acetonitrile containing 0.1% (vol/vol) formic acid] and Solvent B [acetonitrile containing 0.1% (vol/vol) formic acid]; the separation was achieved with a linear gradient of Solvent B from 0.1% to 90% within 10.5 min. The ESI–HRMS conditions were the same as described above except that the parent scan was in the range of *m/z* 700–1200. The authentic standards, coenzyme A (CoA-SH) and benzoyl-CoA, were used to confirm the formation efficiency and investigate the fragmentation patterns of the CoA-esters in the UPLC–ESI–HRMS environment.

RNA extraction of strain B50

Strain B50 was grown in the chemically defined mineral medium (100 ml) supplemented with 1 mM E1, testosterone or cholesterol as the sole carbon source. In brief, 0.8 ml of the stock solution containing 125 mM steroid substrate (in DMSO) was added to the individual bacterial cultures. Bacterial cells were harvested when the substrate was consumed. Cell pellets were resuspended in 200 μl of lysozyme buffer containing 20 mM Tris-HCl, 2 mM EDTA, 1% Triton X-100 and 0.8 mg of lysozyme. After incubation at 37 °C for 1 h, 600 μl of TRI reagent (Sigma-Aldrich) was added into the sample, which was maintained at −80 °C until further RNA extraction. Total RNA was extracted using the Direct-zol RNA MiniPrep kit (Zymo Research, Irvine, CA, USA), and residual DNA was removed using the TURBO DNA-free kit (Thermo Fisher Scientific). The quality and quantity of resulting RNA samples were determined using BioAnalyzer 2100 (Agilent) and Qubit RNA HS assay kit (Thermo Fisher Scientific), respectively, whereas the DNA-removing efficacy was evaluated using the Qubit 1× dsDNA HS assay kit (Thermo Fisher Scientific).

RNA-Seq sequencing of strain B50

Ribosomal RNA was removed from strain B50 transcriptomes by using the Ribo-Zero Magnetic Kit (EPICENTRE Biotechnologies, Madison, WI, USA). Further library construction, including cDNA synthesis, adaptor ligation and enrichment, was performed according to the instruction of the TruSeq Stranded mRNA Library Prep (Illumina, San Diego, CA, USA). The constructed libraries were sequenced as pair-end reads (with a 301-bp read length) on the Illumina MiSeq system (Illumina, San Diego, CA, USA). The strain B50 genome (accession no.: WPAG00000000.1) and transcriptomes were uploaded onto KBase (Arkin *et al.*, 2018). Detailed information and data sets are accessible online (https://kbase.us/n/89341/15/), and the protocol for the transcriptomic analysis is described as follows: Step 1, the strain 50 genome was uploaded and used as a reference genome; step 2, the three transcriptomes (pair-end reads in the FASTQ format) were uploaded using the 'Import FASTQ/SRA File as Reads from Staging Area' application; step 3, the uploaded transcriptomic data were grouped into a RNA-seq data set by using the 'Create RNA-seq Sample Set' application; step 4, forward and reverse reads were merged and trimmed using the 'Trim Reads with Trimmomatic-v0.36' application under the default setting; step 5, this trimmed set was aligned to reference genomes by using HISAT2 and the corresponding application was 'Align reads using HISAT2-V2.1.0'; and step 6, StringTie was used to assemble RNA-seq reads by using the 'Assemble Transcripts using StingTie-v1.3.3b' application. Finally, gene expression under different growth conditions (growth with E1, testosterone, or cholesterol) is shown as fragments per kilobase of transcript per million values in Dataset S1.

Acknowledgements

This study was supported by the Ministry of Science and Technology of Taiwan (109-2221-E-001-002, 109-2811-B-001-513 and 110-2311-B-031-001) and Academia Sinica Career Development Award (AS-CDA-110-L13). Po-Hsiang Wang was supported by the Research and Development Office as well as Research Center for Sustainable Environmental Technology, National Central University, Taiwan. We thank the Institute of Plant and Microbial Biology, Academia Sinica, for providing access to the Small Molecule Metabolomics Core Facility (for UPLC–HRMS analyses). We also thank the NGS High Throughput Genomics Core at BRCAS, Academia Sinica for MiSeq sequencing.

Conflict of interest

The authors have no conflicts of interest to declare.

Author contributions

Y.-R.C. and Y.-L.C. designed the study. T.-H.H., T.-H.L. and M.-R.C. performed the experiments. M.M., M.H. and

T.H. contributed new reagents and analytic tools. Y.-L.C., T.-H.H. and Y.-R.C analysed data. Y.-R.C and P.-H.W. drafted the manuscript. All authors reviewed the manuscript.

References

Arkin, A.P., Cottingham, R.W., Henry, C.S., Harris, N.L., Stevens, R.L., Maslov, S., *et al*. (2018) KBase: the United States Department of Energy systems biology knowledgebase. *Nat Biotechnol* **36:** 566–569.

Balbi, T., Ciacci, C., and Canesi, L. (2019) Estrogenic compounds as exogenous modulators of physiological functions in molluscs: signaling pathways and biological responses. *Comp Biochem Physiol C Toxicol Pharmacol* **222:** 135–144.

Baronti, C., Curini, R., D'Ascenzo, G., Di Corcia, A., Gentili, A., and Samperi, R. (2000) Monitoring natural and synthetic estrogens at activated sludge sewage treatment plants and in a receiving river water. *Environ Sci Technol* **34:** 5059–5066.

Belfroid, A.C., Van der Horst, A., Vethaak, A.D., Schäfer, A.J., Rijs, G.B., Wegener, J., and Cofino, W.P. (1999) Analysis and occurrence of estrogenic hormones and their glucuronides in surface water and waste water in The Netherlands. *Sci Total Environ* **225:** 101–108.

Bergstrand, L.H., Cardenas, E., Holert, J., Van Hamme, J.D., and Mohn, W.W. (2016) Delineation of steroid-degrading microorganisms through comparative genomic analysis. *MBio* **7:** e00166.

Chen, Y.-L., Fu, H.-Y., Lee, T.-H., Shih, C.-J., Huang, L., Wang, Y.-S., *et al*. (2018) Estrogen degraders and estrogen degradation pathway identified in an activated sludge. *Appl Environ Microbiol* **84:** e00001-18.

Chen, Y.-L., Yu, C.-P., Lee, T.-H., Goh, K.-S., Chu, K.-H., Wang, P.-H., *et al*. (2017) Biochemical mechanisms and catabolic enzymes involved in bacterial estrogen degradation pathways. *Cell Chem Biol* **24:** 712–724.

Chiang, Y.R., Wei, S.T.S., Wang, P.H., Wu, P.H., and Yu, C.P. (2020) Microbial degradation of steroid sex hormones: implications for environmental and ecological studies. *Microb Biotechnol* **13:** 926–949.

Coombre, R.G., Tsong, Y.Y., Hamilton, P.B., and Sih, C.J. (1966) Mechanisms of steroid oxidation by microorganisms. X. Oxidative cleavage of estrone. *J Biol Chem* **241:** 1587–1595.

Crowe, A.M., Workman, S.D., Watanabe, N., Worrall, L.J., Strynadka, N.C.J., and Eltis, L.D. (2018) IpdAB, a virulence factor in *Mycobacterium tuberculosis*, is a cholesterol ring-cleaving hydrolase. *Proc Natl Acad Sci USA* **115:** E3378–E3387.

Fujii, K., Kikuchi, S., Satomi, M., Ushio-Sata, N., and Morita, N. (2002) Degradation of 17β-estradiol by a gram-negative bacterium isolated from activated sludge in a sewage treatment plant in Tokyo, Japan. *Appl Environ Microbiol* **68:** 2057–2060.

Gilbert, S., Hood, L., and Seah, S.Y.K. (2017) Characterization of an aldolase involved in cholesterol side chain degradation in *Mycobacterium tuberculosis*. *J Bacteriol* **200:** e00512-17.

Hamid, H., and Eskicioglu, C. (2012) Fate of estrogenic hormones in wastewater and sludge treatment: a review of properties and analytical detection techniques in sludge matrix. *Water Res* **46:** 5813–5833.

Hanselman, T.A., Graetz, D.A., and Wilkie, A.C. (2003) Manure-borne estrogens as potential environmental contaminants: a review. *Environ Sci Technol* **37:** 5471–5478.

Harvey, R.A., and Ferrier, D.R. (2011) *Biochemistry*. Baltimore, MD: Lippincott Williams & Wilkins.

Holert, J., Yücel, O., Jagmann, N., Prestel, A., Möller, H.M., and Philipp, B. (2016) Identification of bypass reactions leading to the formation of one central steroid degradation intermediate in metabolism of different bile salts in *Pseudomonas* sp. strain Chol1. *Environ Microbiol* **18:** 3373–3389.

Hsiao, T.H., Chen, Y.L., Meng, M., Chuang, M.R., Horinouchi, M., Hayashi, T., *et al*. (2021) Mechanistic and phylogenetic insights into actinobacteria-mediated estrogen biodegradation in urban estuarine sediments. *Microb Biotechnol* **14:** 1212–1227.

Huang, C.-H., and Sedlak, D.L. (2001) Analysis of estrogenic hormones in municipal wastewater effluent and surface water using enzyme-linked immunosorbent assay and gas chromatography/tandem mass spectrometry. *Environ Toxicol Chem* **20:** 133–139.

Ibero, J., Galán, B., Díaz, E., and García, J.L. (2019a) Testosterone degradative pathway of *Novosphingobium tardaugens*. *Genes* **10:** 871.

Ibero, J., Galán, B., Rivero-Buceta, V., and García, J.L. (2020) Unraveling the 17β-estradiol degradation pathway in *Novosphingobium tardaugens* NBRC 16725. *Front Microbiol* **11:** 588300.

Ibero, J., Sanz, D., Galán, B., Díaz, E., and García, J.L. (2019b) High-quality whole-genome sequence of an estradiol-degrading strain, *Novosphingobium tardaugens* NBRC 16725. *Microb Resour Annouc* **8:** e01715–e01718.

Jurgens, M.D., Holthaus, K.I.E., Johnson, A.C., Smith, J.J.L., Hetheridge, M., and Williams, R.J. (2002) The potential for estradiol and ethinylestradiol degradation in English Rivers. *Environ Toxicol Chem* **21:** 480–488.

Ke, J., Zhuang, W., Gin, K.Y.H., Reinhard, M., Hoon, L.T., and Tay, J.H. (2007) Characterization of estrogen-degrading bacteria isolated from an artificial sandy aquifer with ultrafiltered secondary effluent as the medium. *Appl Microbiol Biotechnol* **75:** 1163–1171.

Koh, Y.K.K., Chiu, T.Y., Boobis, A., Cartmell, E., Scrimshawm, M.D., and Lester, J.N. (2008) Treatment and removal strategies for estrogens from wastewater. *Environ Technol* **29:** 245–267.

Kolodziej, E.P., Gray, J.L., and Sedlak, D.L. (2003) Quantification of steroid hormones with pheromonal properties in municipal wastewater effluent. *Environ Toxicol Chem* **22:** 2622–2629.

Kolodziej, E.P., Harter, T., and Sedlak, D.L. (2004) Dairy wastewater, aquaculture, and spawning fish as sources of steroid hormones in the aquatic environment. *Environ Sci Technol* **38:** 6377–6384.

Kramer, V.J., Miles-Richardson, S., Pierens, S.L., and Giesy, J.P. (1998) Reproductive impairment and induction of alkaline-labile phosphate, a biomarker of estrogen exposure, in fathead minnows (*Pimephales promelas*)

exposed to waterborne 17β-estradiol. *Aquat Toxicol* **40:** 335–360.

Kurisu, F., Ogura, M., Saitoh, S., Yamazoe, A., and Yagi, O. (2010) Degradation of natural estrogen and identification of the metabolites produced by soil isolates of *Rhodococcus* sp. and *Sphingomonas* sp. *J Biosci Bioeng* **109:** 576–582.

Lee, Y.C., Wang, L.M., Xue, Y.H., Ge, N.C., Yang, X.M., and Chen, G.H. (2006) Natural estrogens in the surface water of shenzhen and the sewage discharge of Hong Kong. *Hum Ecol Risk Assess Int J* **12:** 301–312.

Li, S., Sun, K., Yan, X., Lu, C., Waigi, M.G., Liu, J., and Ling, W. (2021) Identification of novel catabolic genes involved in 17β-estradiol degradation by *Novosphingobium* sp. ES2-1. *Environ Microbiol* **23:** 2550–2563.

Lin, A.Y., and Reinhard, M. (2005) Photodegradation of common environmental pharmaceuticals and estrogens in river water. *Environ Toxicol Chem* **24:** 1303–1309.

Lin, C.-W., Wang, P.-H., Ismail, W., Tsai, Y.-W., El Nayal, A., Yang, C.-Y., *et al*. (2015) Substrate uptake and subcellular compartmentation of anoxic cholesterol catabolism in *Sterolibacterium denitrificans*. *J Biol Chem* **290:** 1155–1169.

Lorenzen, A., Hendel, J.G., Conn, K.L., Bittman, S., Kwabiah, A.B., Lazarovitz, G., *et al*. (2004) Survey of hormone activities in municipal biosolids and animal manures. *Environ Toxicol* **19:** 216–225.

Matsumoto, T., Osada, M., Osawa, Y., and Mori, K. (1997) Gonadal estrogen profile and immunohistochemical localization of steroidogenic enzymes in the oyster and scallop during sexual maturation. *Comp Biochem Physiol B: Biochem Mol Biol* **118:** 811–817.

Noguera-Oviedo, K., and Aga, D.S. (2016) Chemical and biological assessment of endocrine disrupting chemicals in a full scale dairy manure anaerobic digester with thermal pretreatment. *Sci Total Environ* **550:** 827–834.

Pelletier, D.A., and Harwood, C.S. (1998) 2-Ketocyclohexanecarboxyl coenzyme A hydrolase, the ring cleavage enzyme required for anaerobic benzoate degradation by *Rhodopseudomonas palustris*. *J Bacteriol* **180:** 2330–2336.

Pelletier, D.A., and Harwood, C.S. (2000) 2-Hydroxycyclohexanecarboxyl coenzyme A dehydrogenase, an enzyme characteristic of the anaerobic benzoate degradation pathway used by *Rhodopseudomonas palustris*. *J Bacteriol* **182:** 2753–2760.

Qin, D., Ma, C., Lv, M., and Yu, C.P. (2020) *Sphingobium estronivorans* sp. nov. and *Sphingobium bisphenolivorans* sp. nov., isolated from a wastewater treatment plant. *Int J Syst Evol Microbiol* **70:** 1822–1829.

Rabus, R., and Widdel, F. (1995) Anaerobic degradation of ethylbenzene and other aromatic hydrocarbons by new denitrifying bacteria. *Arch Microbiol* **163:** 96–103.

Schaefer, C.M., Lu, R., Nesbitt, N.M., Schiebel, J., Sampson, N.S., and Kisker, C. (2015) FadA5 a thiolase from *Mycobacterium tuberculosis*: a steroid-binding pocket reveals the potential for drug development against tuberculosis. *Structure* **23:** 21–33.

Takamura, Y., and Nomura, G. (1988) Changes in the intracellular concentration of acetyl-CoA and malonyl-CoA in relation to the carbon and energy metabolism of *Escherichia coli* K12. *J Gen Microbiol* **134:** 2249–2253.

Tarrant, A.M., Blomquist, C.H., Lima, P.H., Atkinson, M.J., and Atkinson, S. (2003) Metabolism of estrogens and androgens by scleractinian corals. *Comp Biochem Physiol B Biochem Mol Biol* **136:** 473–485.

Thayanukul, P., Zang, K., Janhom, T., Kurisu, F., Kasuga, I., and Furumai, H. (2010) Concentration-dependent response of estrone-degrading bacterial community in activated sludge analyzed by microautoradiography-fluorescence in situ hybridization. *Water Res* **44:** 4878–4887.

Tian, K., Meng, F., Meng, Q., Gao, Y., Zhang, L., Wang, L., *et al*. (2020) The analysis of estrogen-degrading and functional metabolism genes in *Rhodococcus equi* DSSKP-R-001. *Int J Genomics* **2020:** 9369182.

Wang, P.H., Chen, Y.L., Wei, S.T.S., Wu, K., Lee, T.H., Wu, T.Y., and Chiang, Y.R. (2020) Retroconversion of estrogens into androgens by bacteria via a cobalamin-mediated methylation. *Proc Natl Acad Sci USA* **117:** 1395–1403.

Wu, K., Lee, T.H., Chen, Y.L., Wang, Y.S., Wang, P.H., Yu, C.P., *et al*. (2019) Metabolites involved in aerobic degradation of the A and B rings of estrogen. *Appl Environ Microbiol* **85:** e02223-18.

Yoshimoto, T., Nagai, F., Fujimoto, J., Watanabe, K., Mizukoshi, H., Makino, T., *et al*. (2004) Degradation of estrogens by Rhodococcus zopfii and Rhodococcus equi isolates from activated sludge in wastewater treatment plants. *Appl Environ Microbiol* **70:** 5283–5289.

Yu, C.P., Deeb, R.A., and Chu, K.H. (2013) Microbial degradation of steroidal estrogens. *Chemosphere* **91:** 1225–1235.

Yu, C.P., Roh, H., and Chu, K.H. (2007) 17β-estradiol-degrading bacteria isolated from activated sludge. *Environ Sci Technol* **41:** 486–492.

Yuan, T., Yang, M., Gehring, K., and Sampson, N.S. (2019) *Mycobacterium tuberculosis* exploits a heterohexameric enoyl-CoA hydratase retro-aldolase complex for cholesterol catabolism. *Biochemistry* **58:** 4224–4235.

Zhao, H., Tian, K., Qiu, Q., Wang, Y., Zhang, H., Ma, S., *et al*. (2018) Genome analysis of *Rhodococcus* Sp. DSSKP-R-001: A highly effective β-estradiol-degrading bacterium. *Int J Genomics* **2018:** 3505428.

Supporting information

Additional supporting information may be found online in the Supporting Information section at the end of the article.

Table S1. Olig onucleotides used in this study.

Fig. S1. Deduced amino acid sequence alignments (A) and phylogenetic tree (B) of the aldolase and thiolase genes involving in actinobacterial steroid catabolism. (A) The alignment was performed using the software Jalview version 2.11.1.4 with Muscle under default. Residue similarities between individual sequences are present in purple gradient according to the BLOSUM62 scores. Active and binding sites of the characterized enzymes (Ltp2 and FadA5) are highlighted with green or red backgrounds, respectively. (B) The enzyme phylogeny is shown in a neighbour joining tree. Ltps and FadA5 sequences are available in the UniprotKB

with the Entry of I6Y3T7 and I6XHI4. Locus tag numbers of aedK: GMFMDNLD_05342 and C7H75_RS25375; locus tag numbers of aedF: GMFMDNLD_05335 and C7H75_RS25410.

Fig. S2. Alignment of the MaoC-like sequences involving in actinobacterial steroid degradation. The alignment was performed using the software Jalview version 2.11.1.4 with Muscle under default. The residue similarities between individual sequences are present in purple gradient, according to the BLOSUM62 scores, The DUF35 domain is enclosed in a black box. ChsH2 sequences are available in the UniprotKB with the Entry of I6YGF8. Locus tag numbers of the aedL genes: GMFMDNLD_05343 (strain B50) and C7H75_RS25370 (strain DSSKP-R-001).

Fig. S3. Geneticmaps of the complementation constructs for three estrogen degradation genes *aedF* (A), *aedK* (B), and *fadD3* (C).

Fig. S4. ESI–HRMS spectra of three novel estrogenic metabolites produced by strain B50.

Fig S5. ^{1}H-(500 MHz) (A) and ^{13}C-NMR (125 MHz) (B) spectra of Metabolite **2**.

Fig. S6. ^{1}H-(500 MHz) (A) and ^{13}C-NMR (125 MHz) (B) spectra of Metabolite **3**.

Fig. S7. ^{1}H-(500 MHz) (A) and ^{13}C-NMR (125 MHz) (B) spectra of Metabolite **7**.

Fig. S8. COSY (A) and HMBC (B) spectra of Metabolite **2**.

Fig. S9. COSY (A) and HMBC (B) spectra of Metabolite **3**.

Fig. S10. COSY (A) and HMBC (B) spectra of Metabolite **7**.

Fig. S11. The uncropped full-range agarose gel (1%) of Fig. 3Bi.

Fig. S12. The uncropped full-range agarose gel (1%) of Fig. 3Bii.

Dataset S1. The genome and transcriptomes (RNA-Seq) of strain B50 grown with estrone, testosterone, or cholesterol.

